Ruggedized Optical Fiber Sensors for Downhole Monitoring

Russell G. May (rmay@vt.edu; 540-231-1837)
Anbo Wang (awang@vt.edu; 540-231-4355)
Hai Xiao (hxiao@vt.edu; 40-231-7070)
Jiangdong Deng (jdeng@vt.edu; 540-231-3829)

Photonics Laboratory
Bradley Department of Electrical and Computer Engineering
Virginia Tech
Blacksburg, VA 24061-0111

Contract Information: This research was sponsored by the U.S. Department of Energy's Federal Energy Technology Center, under Contract DE-FG26-988C15167 with the Virginia Polytechnic Institute and State University, Blacksburg, VA, and in collaboration with Chevron Research and Technology Company.

Introduction

Efficient and complete recovery of petroleum reserves is difficult in part due to a lack of robust instrumentation for characterization of physical conditions in the downhole environment. Accurate evaluation of pressure, temperature, and volumetric flow would permit optimization of oil recovery processes. Unfortunately, sensors currently used for downhole characterization have demonstrated limited lifetimes in the harsh environment that are typical for this application. Development of ruggedized instrumentation engineered specifically for the downhole environment will accelerate the adoption of technology leading to intelligent completions.

Under the sponsorship of the U.S. Department of Energy National Petroleum Technology Office, and in collaboration with Chevron Research and Technology Company, the Photonics Laboratory at Virginia Tech is investigating the application of optical fiber sensor technology to the development of ruggedized sensors for the downhole environment. Using a new sensor configuration which has been labeled the Self-Calibrating Interferometric/Intensity-Based (SCIIB) sensor, designs for the measurement of pressure, temperature, flow, and acoustic waves are being evaluated. The SCIIB configuration combines the best features of both interferometric and intensity-based optical sensors, resulting in a sensor that demonstrates the high sensitivity of interferometry, together with the simple signal processing of intensity-based sensors. In addition, the sensor probe generates two signals, which can be combined to realize self-calibrating operation. Undesired perturbations such as fluctuations in the optical source power or losses due to bends in the optical fiber are common-mode. Ratiometric processing of the two signals eliminates the common-mode perturbations and yields the desired measurand. Tests, as described below, have shown that the SCIIB sensor has a low cross-sensitivity to undesired physical effects.

Objective

Measurement and characterization of physical conditions in the downhole oil production environment will not only enable adoption of completion strategies based on expanded data from recovery processes, but also provide enhanced characterization of existing reserves. To this end, the objective of this research program is to develop and evaluate sensors for downhole measurement of pressure, temperature, volumetric flow, and acoustic waves (for seismic applications), and to develop technology to enable survival of the sensors over extended periods of time. This paper describes preliminary research in the development of a miniaturized fiber optic pressure sensor for downhole use.

Approach

Several methods have been demonstrated for the measurement of physical phenomena using optical fiber sensors. In general, some parameter of the lightwave guided by the optical fiber is modified by the measurand, and the magnitude of the measurand is inferred from the amount of change of the lightwave parameter. Some of the changes in the lightwave that can be related to applied external effects include changes in intensity (optical power), wavelength, phase, and polarization. Of these, sensors employing either changes in lightwave intensity or phase have been the most widely researched.

Intensity-based sensors are relatively simple to implement. Low-cost light sources such as light emitting diodes (LEDs) can be used, and simple photodetectors may be employed to determine the intensity of the optical power in the sensor output. An example of one type of intensity-based fiber optic sensor configured as a pressure sensor is a microbend sensor, shown in Figure 1a. A length of optical fiber connecting a source and detector is sandwiched between two plates in which ridges have been machined. When a pressure is applied to one of the plates, the resulting force deforms the fiber in a quasi-sinusoidal pattern. From experience with the design of optical fiber cables for telecommunication, it is well known that periodic deformations of an optical can generate sizable optical losses, even if the amplitude of the deformation is only a small fraction of the fiber diameter. Therefore, the pressure applied to the plate can be correlated to the reduction in optical power transmitted through the fiber, either through theoretical analysis or by experimental calibration.

However, other effects can also cause a reduction in the optical power output by the sensor, resulting in possible misinterpretation of the change as due to applied pressure. For example, bends in the optical fiber connecting the source to the sensor, which may result from routing the fiber around an obstacle, generate attenuation in the fiber. This reduction in optical power transmitted through the fiber may be erroneously interpreted as an increase in pressure applied to the sensor. In as similar manner, fluctuations in the power output by the optical source, perhaps arising from changes in the temperature of the source, also result in a change in the power incident on the photodetector. Again, the change in optical power spoofs a change in the applied pressure.

In contrast, interferometric fiber optic sensors, in which the measurand produces a change in the phase of the lightwave, are largely insensitive to optical losses in the fiber. In a typical inteferometric sensor, light from a source with high coherence, such as a laser diode, is split into two paths. One type of fiber optic interferometer, a Mach-Zehnder, is illustrated in Figure 1b. One path (the reference leg) is isolated from the physical effect to be measured, while the other (the sensor leg) is subjected to the effect. The sensor is engineered so that the applied measurand effects a change in the optical path length of the sensor leg, either by elongation of the leg, or by a change in the refractive index of the leg. In the example shown, pressure applied to matched plates generates a deformation in the fiber, which elongates the fiber. At the output of the sensor, the light in the two legs is combined. Since the light is coherent, the two paths interfere, with the state of the interference depending on the relative phase difference between the interfering lightwaves; if the waves are in phase, they interfere constructively, producing strong optical power, and if they are out of phase, they interfere destructively, with a reduction in optical power.

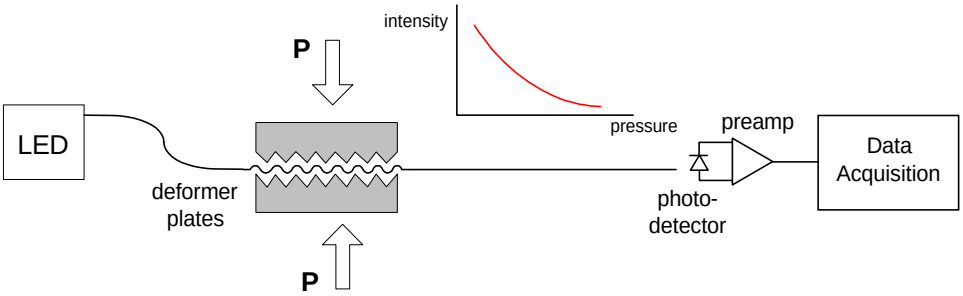

Figure 1a. Fiber optic intensity-based sensor for the measurement of pressure through microbends.

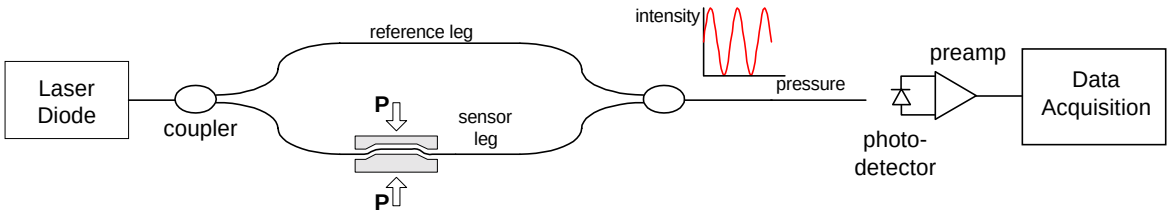

Figure 1b. Fiber optic interferometric sensor for the measurement of pressure through elongation of fiber.

Figure 2 displays the output intensity of a typical interferometric sensor as a function of the change in optical path length (the product of the physical length and the refractive index of the sensor leg). Since the interferometer output changes dramatically for changes in optical path length of less than the wavelength of light (on the order of 10^{-6} meter), the interferometer yields highly sensitive measurements of fiber elongation or

refractive index change. However, as the figure illustrates, changes in optical path length longer than a wavelength yields periodic changes in the power output by the sensor. The term commonly used for each peak in intensity is a “fringe.” The periodic output of the interferometer complicates the interpretation of the output, requiring additional equipment or algorithms to yield an output that is a monotonically varying function of the applied pressure. Some of the techniques used include counting of fringes, and use of more than one wavelength to derive an unambiguous measurement of the interference state.

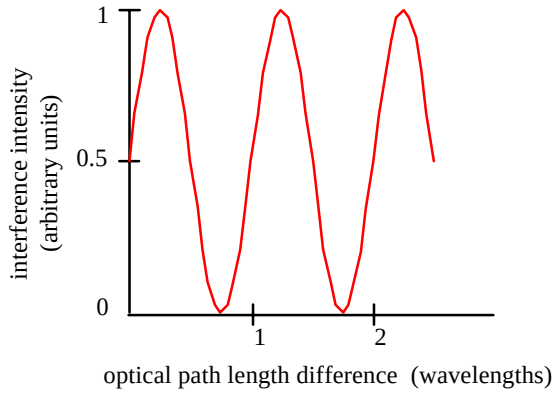

Figure 2. Typical output of an interferometric sensor for an increase in optical path length.

The Self-Calibrating Interferometric/Intensity-Based (SCIIB) sensor configuration, recently invented at the Virginia Tech Photonics Laboratory, combines the high sensitivity of interferometry with the simple signal processing of intensity-based sensors. The sensor, illustrated in Figure 3, employs a structure known as a Fabry-Perot interferometer cavity, formed by aligning two polished fiber ends inside a capillary tube. When light is injected into the sensor’s input fiber, it propagates through the fiber until it reaches the end of the fiber. Due to the discontinuity in refractive index, approximately 4% of the optical power is reflected at the fiber end as a result of Fresnel reflections (reflection R_1 in the figure). The remaining 96% of the light continues across the air gap of the cavity, until 4% of that light is reflected from the end of the second (reflector) fiber. This second reflection (R_2) travels back across the air gap and into the first (input) fiber, where it combines with the first reflection. If the optical source is coherent enough, the reflections interfere, and the intensity of the optical output of the sensor depends on the relative phase difference of the two reflections.

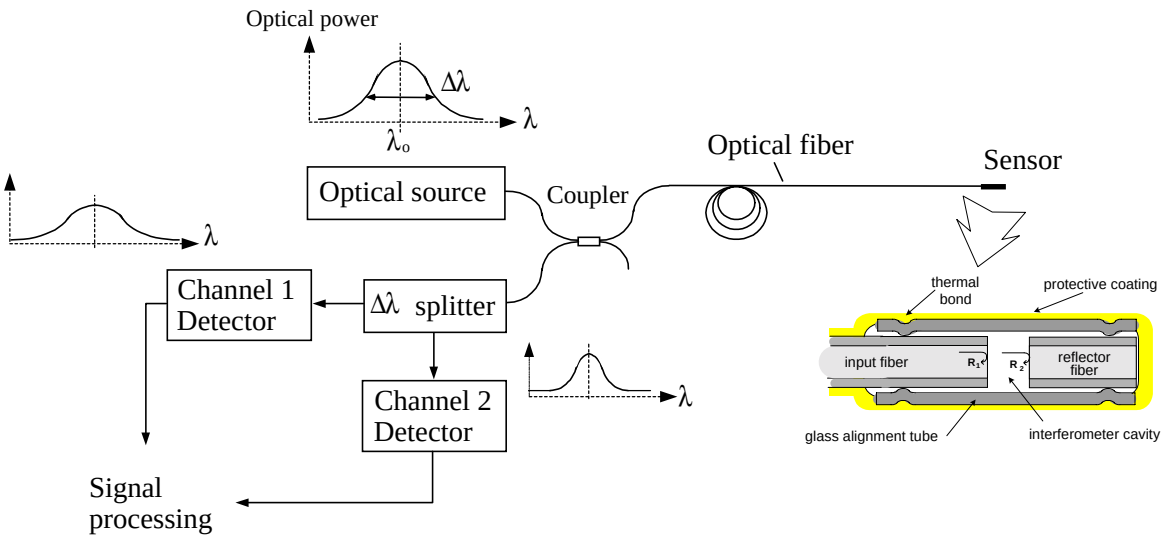

Figure 3. Schematic of Self-Calibrating Interferometric/Intensity-Based (SCIIB) sensor system, showing detail of sensor configured as a pressure sensor.

For the configuration presented in Figure 4, hydrostatic pressure applied to the sensor probe results in a deformation of the glass capillary alignment tube. When the applied pressure exceeds the pressure of the air trapped in the sensor, the radius of the tube decreases, causing an increase in the separation of the two fibers. From the principles of mechanics, an analytical expression relating the change ΔL in air gap separation to the applied pressure p is found to be

$$\Delta L = \frac{L p r_o^{\,2}}{E(r_o^{\,2} - r_i^{\,2})}(1-2\mu) \qquad (1)$$

where

p is the applied pressure,
μ is the Poisson's ratio of the glass, and
E is the Young's modulus of the glass.

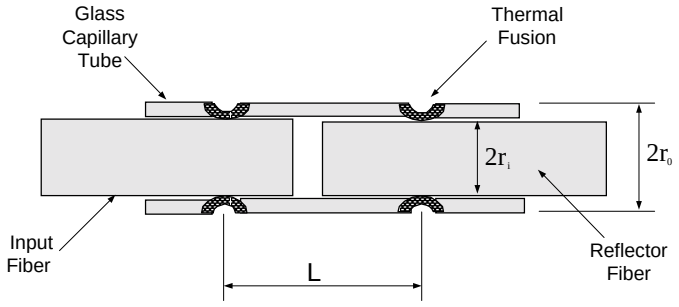

Figure 4. Schematic illustrating geometry of SCIIB pressure sensor.

To simplify the processing and interpretation of the sensor output, the sensor probe is designed so that the optical intensity of the output over the expected full range of the applied pressure remains within the quasi-linear part of the sinusoidal output. This is accomplished by controlling the length, diameter, wall thickness, and the modulus of elasticity of the capillary alignment tube during sensor fabrication. When properly designed, the excursion ΔL of the gap during the application of pressure can be limited so that the sensor output is constrained to the quasi-linear portion of the interferometric function, corresponding to the bold highlight in Figure 5. In this way, complicated signal processing involving fringe counting or spectral decomposition can be avoided, and a simple photodetector may be used, since the optical power output is then linearly related to the applied pressure through Equation 1.

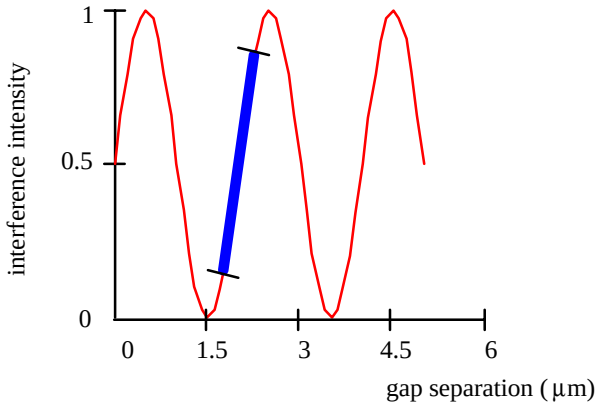

Figure 5. Intensity output of Fabry-Perot cavity, highlighting the quasi-linear region of the sensor output.

However, since the sensor's output signal is now processed like an intensity-based sensor, changes in the attenuation of the input fiber or in the output power of the source may generate errors. To eliminate this possibility, an optical beamsplitter is used to split the sensor output into two channels. Optical filters are then used to adjust the coherence of the light in the two channels. In the reference channel, the light is adjusted to have a short coherence length; in the sensor channel, the light is changed to have a long coherence length.

When the coherence length of the light source is longer than the path length difference of the two legs in an interferometer, interference is observed when the light from the two legs are combined. Conversely, when the source coherence length is less than the path length difference, interference does not take place, and the result of combining the two beams is that their intensities add arithmetically. In the SCIIB system, the coherence length of the sensor channel (Channel 2 in Figure 3) is engineered to exceed the path length difference in the Fabry-Perot cavity (the path length difference is twice the gap length, since the reflection R_2 in Figure 3 has to traverse the gap twice). Therefore, the output of Channel 2 will exhibit interference fringes as the gap length is changed due to

changes in applied pressure. As explained above, the output of the sensor channel will be constrained so that the output will be a linear function of pressure. However, changes in bends or connectors in the input fiber will also yield changes in the output of the signal channel. The function of the reference channel is to eliminate these undesired changes.

The coherence length of the reference channel (Channel 1 in Figure 3) is adjusted to be much shorter than the path length difference in the Fabry-Perot cavity; therefore no interference takes place in the output of the reference channel. The power output by Channel 1 is therefore only the sum of the optical power of the two reflections R_1 and R_2, with no interference. The power of those reflections, however, is affected by changes in loss of the fiber or connectors. So both the sensor channel and the reference channel exhibit changes in output due to fiber loss, connector loss, or fluctuations in source output power; only the sensor channel exhibits changes in output due to gap length changes from pressure. The undesired fluctuations in power are common-mode to both signal and reference channels. By taking the ratio of the outputs of the two channels, the undesired fluctuations are canceled out, leaving only the interferometric variations, which contain the desired information about pressure measurements.

Figure 6 contains two plots generated by a theoretical simulation of the SCIIB system, and show the optical power outputs of both the reference and sensor channels. In this example, an optical source with a peak wavelength of 850 nm is assumed. The top plot, corresponding to the reference channel with an optical bandpass of 70 nm, shows that

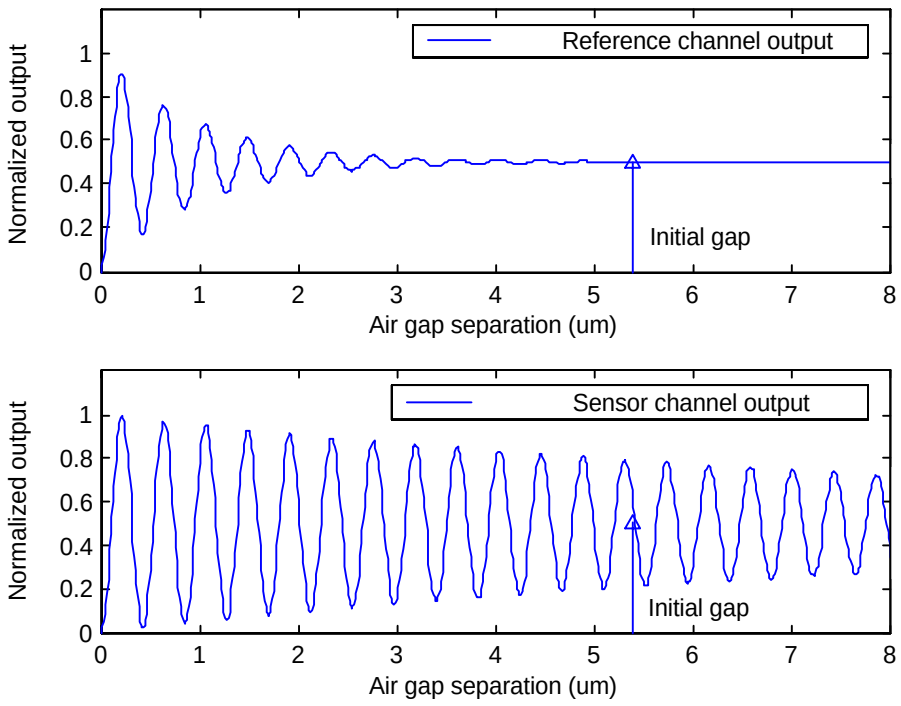

Figure 6. Outputs of two SCIIB channels, demonstrating the difference in interference effects due to coherence filtering.

interference effects are rapidly diminished as the gap increases from zero to a few microns. For gaps greater than five microns, interference effects are absent, and the output intensity equals the sum of the intensities of the two reflections R_1 and R_2. Therefore, for the source assumed for this analysis, the initial gap of the SCIIB Fabry-Perot cavity should be set to at least 5 μm. In contrast, the sensor channel output, with a bandpass of 10 nm, exhibits strong interference effects over the entire range of air gap shown.

Results

To test the validity of the sensor system, a prototype SCIIB pressure sensor was fabricated using a one centimeter long silica tube to form a gap between two single-mode optical fibers. The optical fibers had cladding diameters of 125 μm with core diameters of 62.5 μm, and the silica tube had an inner diameter 130 μm. The outside diameter of the tube was 365 μm. The tube was bonded to the fibers by using a carbon dioxide laser to fuse the glass elements. Using a deadweight pressure calibrator, hydrostatic pressures up to 5000 psi were applied to the probe after it was connected to a laser diode and photodetector. By measuring the output intensity and counting the number of interferometric fringes in the output, the gap displacement could be determined within an accuracy of 0.1 μm. In Figure 7, the measured gap of the sensor probe as the pressure was varied is compared with the gap change predicted by Equation 1. The close match confirms that the change in gap can be used to determine the applied hydrostatic pressure. The discrepancies at higher pressures probably result from the estimate used for the value of Young's modulus of the tube in Equation 1.

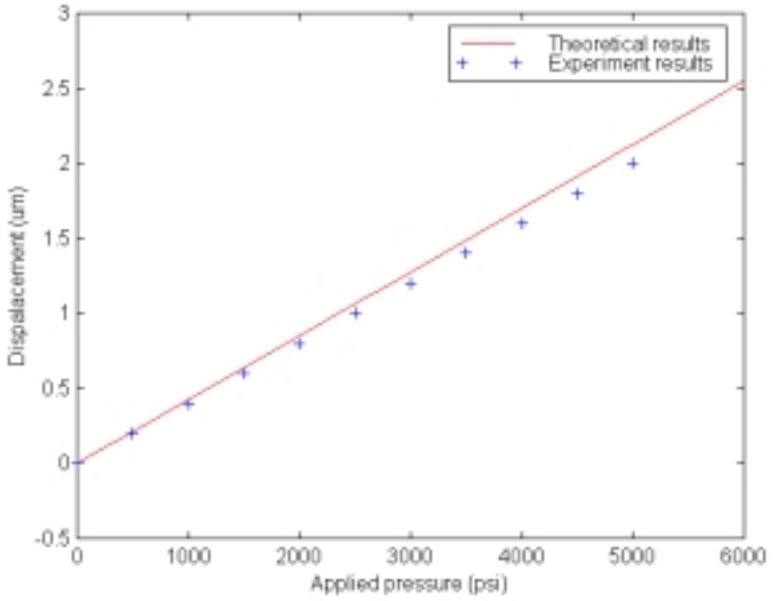

Figure 7. Comparison of experimental results with analytically predicted results for SCIIB pressure sensor.

To test the cross-sensitivity of the SCIIB pressure sensor to temperature, a new sensor was fabricated using 62.5/125 μm (core/cladding) optical fiber inside a 130/365 μm (inside diameter/outside diameter) glass capillary tube. The tube was thermally fused to the fibers so that the distance separating the fused points (parameter *L* in Equation 1) was 630 μm. The sensor was then connected to a two-channel optoelectronic system, similar in design to the system illustrated in Figure 3. An analog-to-digital converter was used to digitize the outputs of the two SCIIB channels, and a personal computer was then employed to calculate the ratio of the sensor channel to the reference channel. Using the deadweight pressure calibrator, the sensor probe was subjected to hydrostatic pressures varying from 0 to 2000 psi. The applied pressure was limited in this test to constrain the sensor output to remain within its quasi-linear region.

The output of the SCIIB system was compared with the pressure applied by the deadweight calibrator to determine the calibration constant for the sensor. Next, the pressure vessel of the calibrator was wrapped with electrical heating tape, so that the temperature applied to the sensor could be varied during the pressure test. A thermocouple was used to monitor the temperature. The temperature was adjusted to 50°C, 100°C, 145°C, and 196°C, in turn. At each temperature, the hydrostatic pressure was increased from 0 to 2000 psi in steps of 100 psi, with the output of the SCIIB sensor recorded for each pressure increment. Figure 8 displays the result of the tests at the four temperatures, and indicates that the temperature changes have an almost negligible effect on the sensor output. The temperature effect was calculated to be 0.04% $°C^{-1}$ over the full range of the sensor output.

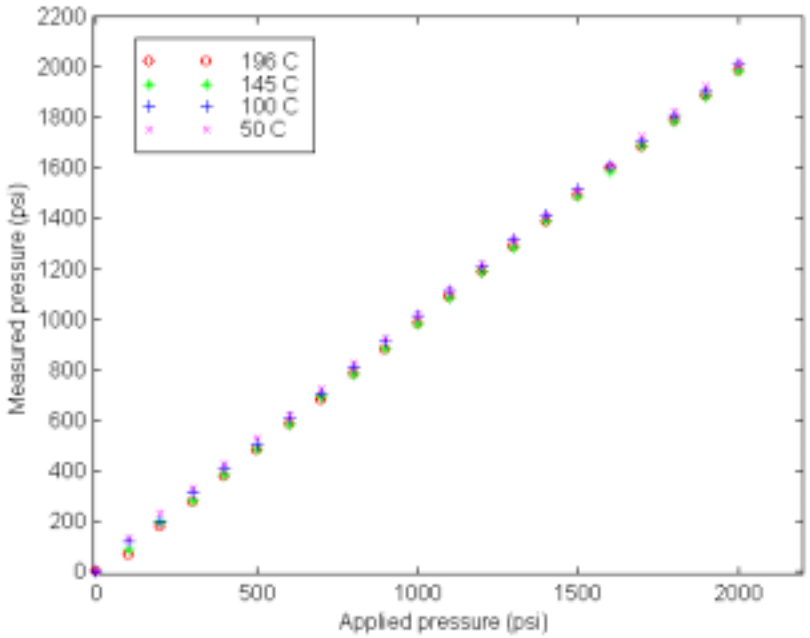

Figure 8. Output of SCIIB pressure sensor for applied pressure at different temperatures.

An experiment was undertaken to investigate the SCIIB system's ability to compensate for undesired changes in the fiber loss or source power. For this test, a 62.5/125 μm (core diameter/cladding diameter) multimode fiber was connected to a two-channel optoelectronic system similar to the one illustrated in Figure 3. The free end of the fiber was not terminated with a Fabry-Perot cavity; in this way, the reflection from the end of the fiber would be absent of interference effects. Under these conditions, the output of the SCIIB system should be constant, even if the source optical power or the fiber attenuation is changed.

To generate a change in the optical loss of the fiber, it was wrapped one turn around a cylindrical mandrel to induce bend losses. Since the magnitude of the optical loss increases as the radius of the bend in the fiber decreases, it is possible to introduce varying amounts of loss by using mandrels of different diameters. The amount of loss induced was calculated by measuring the voltage output by the reference channel when the fiber was bent. This measurement was divided by the output of the reference channel recorded before the fiber was bent. After subtraction of this ratio from a value of one, the loss was then expressed as a normalized value,

$$normalized\ \ fiber\ loss = 1 - \frac{P_{bent}}{P_{straight}}. \qquad (2)$$

The output of the SCIIB system, found by taking the ratio of the two channels, was plotted as a function of normalized fiber loss as the loss was increased from zero to 0.5 (3dB). The results in Figure 9 indicate that the SCIIB system is very effective in rejecting changes in optical power that are common mode to both the reference and sensor channels.

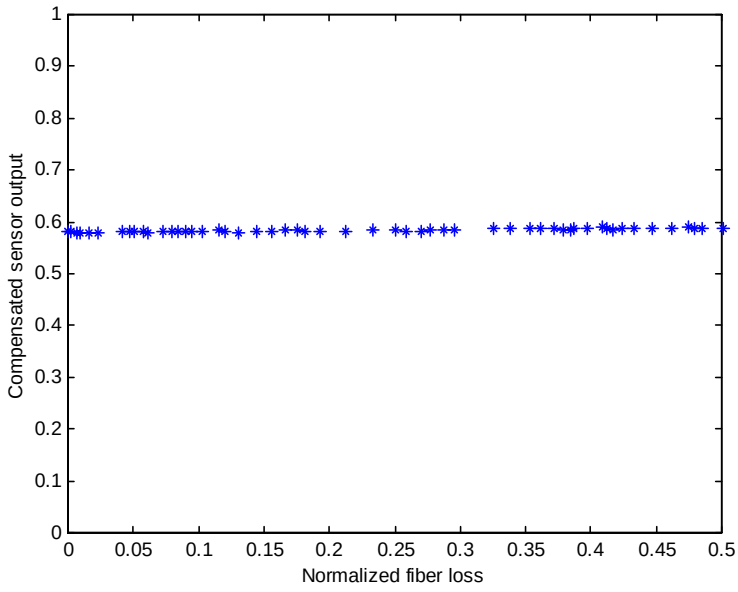

Figure 9. Plot of SCIIB system output as fiber loss was increased up to 3 dB through bending of input fiber.

Future Activities

While the preliminary results presented here validate the optical principles of the SCIIB sensor and suggest a promising future for the application of the sensor in the oil industry, much work remains before the sensor could be considered practical for downhole applications. Currently, our laboratory is developing methods for the automated assembly of the pressure sensor probe. Computer controlled fabrication is expected to enhance sensor repeatability and reliability.

The downhole environment is a particularly harsh one for glass fibers. Water, present in many wells, attacks the amorphous network in silica-based glass, and promotes failure of the fiber through stress corrosion. The high pressures and temperatures present in the downhole environment will only serve to accelerate this process. The polymers that are typically used to coat optical fibers for telecommunications uses are permeable to water under high pressures, due to free volume in the polymers. One of the goals of this research program is to identify coatings that will protect the glass fiber in high-temperature, high-pressure environments. Towards this end, we will evaluate commercially available polymer, metallic, and ceramic coatings for optical fibers, as well as experimental coatings that can be applied to the fibers using Virginia Tech's optical fiber draw tower.

Prototype sensors will be tested in the latter part of the program, first at the University of Tulsa in conditions simulating a typical downhole environment, and then in an actual well in Chevron's Coalinga, CA oil field.

Acknowledgement

The authors gratefully acknowledge the Contracting Officer's Representative, James L. Barnes, of the National Petroleum Technology Office.